ELSEVIER

International Journal of Mass Spectrometry 199 (2000) 235–252

International Journal of Mass Spectrometry

Low energy fragmentation of protonated glycine. An ab initio theoretical study[1]

Françoise Rogalewicz, Yannik Hoppilliard*

Département de Chimie, Laboratoire des Mécanismes Réactionnels, UMR CNRS 7651, Ecole Polytechnique, 91128 Palaiseau Cedex, France

Received 13 October 1999; accepted 3 January 2000

Abstract

A common fragmentation of protonated α-amino acids is the loss of 46 u corresponding to the formation of an immonium ion. From protonated glycine, the fragmentation pathways leading to the loss of 46 u were investigated by means of ab initio calculations at various levels of theory: B3LYP/6-31G*, MP2(FC)/6-31G*, MP2(FC)/6-311+G(2d,2p)//MP2(FC)/6-31G*, and MP2(FC)/6-311+G(2d,2p)//MP2(FC)/6-31G*+ZPVE(MP2(FC)/6-31G*. Several neutral species may correspond to 46 u: formic acid (HCOOH), carbon dioxide and dihydrogen (CO_2 + H_2) from N-protonated glycine; dihydroxycarbene [$C(OH)_2$] from the CO-protonated isomer; and water and carbon monoxide (H_2O + CO) from the OH-protonated form. The difference in energy between the N-, CO-, and OH-protonated forms is calculated to be 0, 112, and 122 kJ mol^{-1} at the highest level of theory. The fragmentation of lowest critical energy is the consecutive loss of water and carbon monoxide that was the mechanism previously admitted. For ions having long lifetimes this reaction is in competition with a loss of CO. This fragmentation and the consecutive losses of H_2O + CO arise through the same determining step that is the isomerization of N-protonated glycine [$GlyH^+$(N)] into OH-protonated glycine located 153 kJ mol^{-1} higher than $GlyH^+$(N). At high energy, the loss of dihydroxycarbene may occur. Its formation from N-protonated glycine requires 313 kJ mol^{-1}. The fragmentation is preceded by an isomerization of N-protonated glycine into CO-protonated glycine. Elimination of formic acid is ruled out by the present calculations. (Int J Mass Spectrom 199 (2000) 235–252) © 2000 Elsevier Science B.V.

Keywords: Ab initio MO calculations; Low energy collisions; Protonated glycine

1. Introduction

The loss of 46 u leading to an immonium ion is a classical and well known fragmentation of energized protonated α-amino acids (see examples in [1–16]). The elemental composition associated with this loss of 46 u is [C, H_2, O_2]. This composition may correspond to several chemical formulae: (1) formic acid (HCOOH); (2) carbon dioxide and dihydrogen (CO_2 + H_2); (3) dihydroxycarbene [$C(OH)_2$]; and (4) water and carbon monoxide (H_2O + CO). The mechanism currently admitted is the consecutive loss of water and carbon monoxide. Arguments in favor of this pathway come from either thermochemical data or mass spectrometric results [4,6,7]. However, in a

* Corresponding author. E-mail: yannik@dcmr.polytechnique.fr

[1]Dedicated to Henri Edouard Audier, on the occasion of his 60th birthday. You are one of the pioneers in the field of mass spectrometry and especially in the field of chemistry in the gas phase. One of us, YH, was your first student. She thanks you very much for having passed your love of mass spectrometry on to her.

PII S1387-3806(00)00189-5

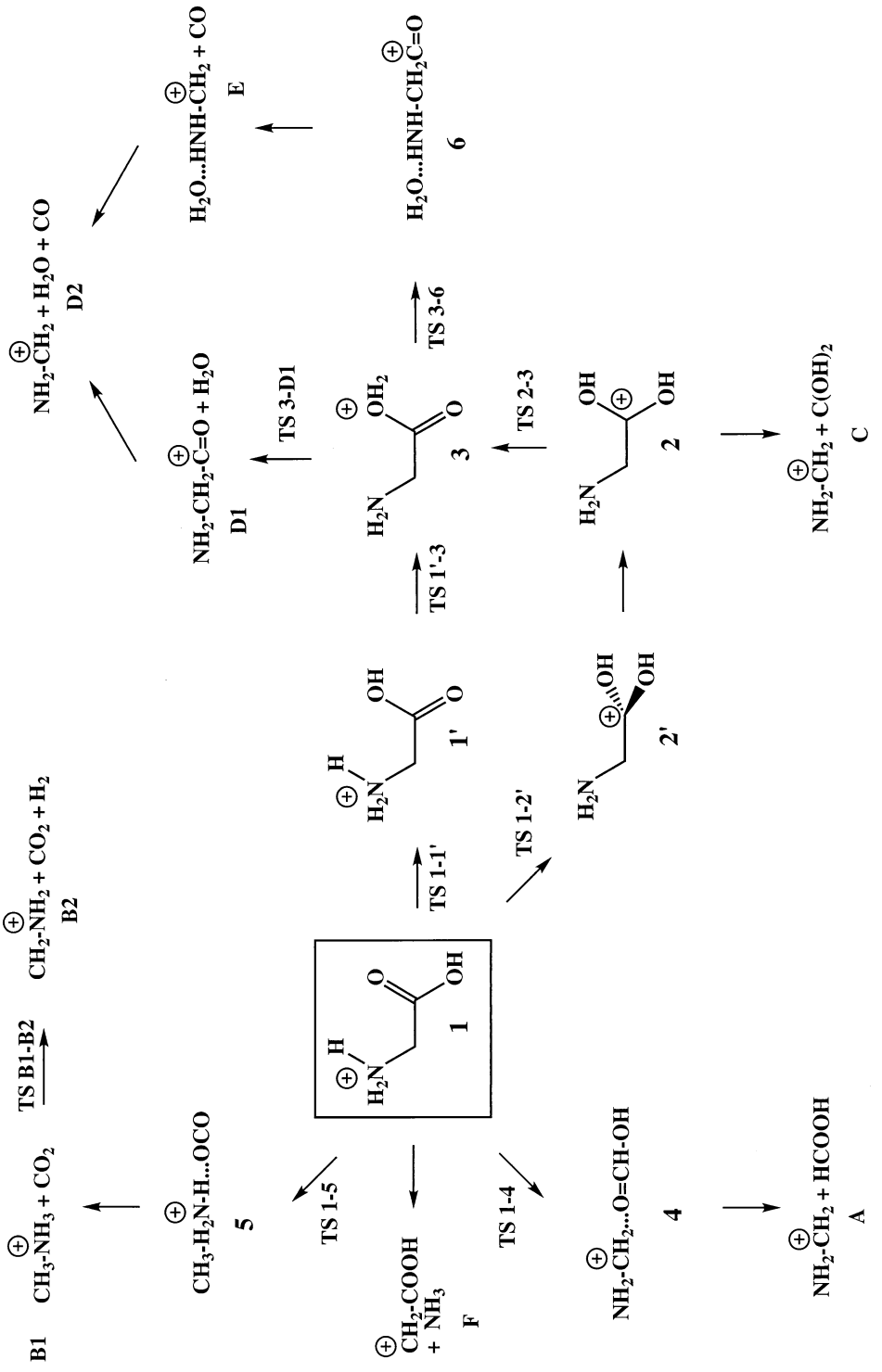
B1
CH3-NH3 + CO2
TS B1-B2
CH2-NH2 + CO2 + H2
B2
5
CH3-H2N-H...OCO
TS 1-5
TS 1-1'
TS 1-2'
TS 1-4
1
1'
2'
2
3
4
TS 1'-3
TS 2-3
TS 3-D1
TS 3-6
F
CH2-COOH + NH3
NH2-CH2...O=CH-OH
NH2-CH2 + HCOOH
A
NH2-CH2-C=O + H2O
D1
NH2-CH2 + CO + H2O
D2
H2O...HNH-CH2-C=O
6
H2O...HNH-CH2 + CO
E
NH2-CH2 + C(OH)2
C

Scheme 1.

recent study, Wesdemiotis et al. [13] examined the neutral mixture liberated upon high energy collisions of protonated glycine ($GlyH^+$) and its isotopomers. They showed that the neutral fragment reionization mass spectrum of $GlyH^+$ includes ions at *m/z* 18, 28, 44, and 46 corresponding to $H_2O^{\cdot+}$, $CO^{\cdot+}$, $CO_2^{\cdot+}$, and $[CH_2O_2]^{\cdot+}$, respectively. These results would suggest that at high collision energy several mechanisms are in competition for the loss of 46 u. As may be expected the neutral species involved in this loss would depend on the internal energy content of protonated amino acids.

The purpose of this work is to investigate, by means of ab initio calculations, the different methods of fragmentation leading to the loss of 46 u and to define the energetic conditions required to observe competitive mechanisms from $GlyH^+$. The potential energy surface (PES) associated with this fragmentation, described in Scheme 1, was calculated at different levels of theory and up to MP2(FC)/6-311+G(2d,2p)// MP2(FC)/6-31G*+ZPVE(MP2(FC)/6-31G*).

This article is divided into two parts. The first is devoted to the protonation of neutral glycine. The geometries of the most stable structures of neutral glycine and of glycine protonated on different basic sites are investigated. The proton affinity of each basic site is evaluated by the difference in total energy, at the highest level of theory, between the most stable conformer of neutral glycine and the most stable form of each isomer of protonated glycine. In the second part the different methods of fragmentation of $GlyH^+$ leading to the loss of 46 u are investigated. The global energy associated with each specific method of decomposition is compared with the critical energy associated with the loss of NH_3, a fragmentation often observed from many protonated amino acids, but not observed in the case of $GlyH^+$.

The relative energies of initial, transition, and final states calculated at various levels of theory are given in Table 1.

2. Computational

All geometry optimizations were carried out at the B3LYP/6-31G* and MP2(FC)/6-31G* levels, without any symmetry constraint. The B3LYP/6-31G* and MP2(FC)/6-31G* levels were used for vibrational frequency calculations. Core orbitals frozen in the MP2 calculations were the 1*s* of C, N, and O. The GAUSSIAN 94 package [17] was used throughout. The B3LYP density functional approach was employed in order to compare the geometries and the relative energies of the species in the PES of $GlyH^+$ obtained with this method to those generated using a classical MP2 ab initio procedure. A comparable reliability of both methods would lead to use of the B3LYP method (significantly less time consuming) for later studies of the PES of larger protonated amino acids and of protonated peptides. In the text the difference in geometry between the MP2 and B3LYP optimizations will be given only when the difference in bond length exceeds 0.2 Å and the difference in valence angle value is higher than 2 °. For many of the minima investigated, several conformations were computed. Results will only be described for the most stable conformer of each species. Transition states were identified as stationary points with one imaginary frequency. The appropriate nature of the transition vector was identified by graphical animation using either the MOLDEN [18] or XMOL [19] programs. The relative energies of initial, transition, and final states were calculated at the following levels of theory: B3LYP/6-31G*, MP2(FC)/6-31G* (MP2/SB), MP2(FC)/6-311+G(2d,2p)//MP2(FC)/6-31G* (MP2/LB), and MP2(FC)/6-311+G(2d,2p)//MP2(FC)/6-31G*+ZPVE(MP2(FC)/6-31G*) (MP2/LB+ZPVE) and are given in Table 1. Except otherwise stated, the relative energies mentioned in the text are those computed at the highest level of theory and the geometries given in Schemes 2–7 are optimized at the MP2/6-31G* level.

3. Results

3.1. Structures and energies of the isomeric protonated forms of glycine

The zwitterionic form of glycine does not appear to exist in the gas phase. Experimentally, the gas-phase

Table 1
Relative energies (kJ mol^{-1}) of the different states associated with the formation and decomposition of $GlyH^+$ calculated at the following levels of theory: B3LYP/6-31G*, MP2(FC)/6-31G*, (MP2/SB), MP2(FC)/6-311+G(2d,2p)//MP2(FC)/6-31G* (MP2/LB), and MP2(FC)/6-311+G(2d,2p)//MP2(FC)/6-31G*+ZPVE(MP2(FC)/6-31G*. The N-protonated form of glycine is taken as the reference

Name	ΔE B3LYP/6-31G*	ΔE MP2/SB	ΔE MP2/LB	ΔE MP2/LB+ZPVE
Protonated molecules and isomeric complexes				
1	0	0	0	0
1′	22	16	18	18
2	120	142	119	112
2′	124	149	124	118
3	179	174	144	122
4	67	85	83	72
5	−76	−88	−76	−81
6	117	92	66	40
Final states				
A = **I** + HCOOH	137	145	142	125
B1 = $CH_3NH_3^+ + CO_2$	−38	−51	−41	−44
B2 = **I** + $H_2 + CO_2$	134	118	136	86
C = **I** + $C(OH)_2$	338	358	333	313
D1 = acylium + H_2O	213	186	146	112
D2 = **I** + H_2O + CO	238	208	167	129
E = $H_2O \cdot HNHCH_2^+CO$	135	109	84	75
F = $NH_3 + {}^+CH_2COOH$	362	376	352	326
Transition states				
TS1-2′	73	172	141	133
TS1-1′	22	32	31	32
TS1′-3	196	164	169	153
TS2-3	332	347	327	302
TS1-4	407	436	403	378
TS1-5	328	343	325	305
TS3-6	189	180	148	125
TS3-D1	187	183	152	127
TSB1-B2	352	359	332	298

acidity and basicity of glycine and several of its methyl-substituted isomers were measured by ion cyclotron resonance mass spectrometry [20]. These data provide convincing chemical evidence that, in the gas phase, glycine is not a zwitterion. Theoretically, the neutral form is computed to be more stable by 71 kJ mol^{-1} (MP2/DZP++//RHF/6-31G*) [21] and at accurate levels of theory the zwitterion is no longer a minimum energy structure in the PES of glycine [21,22]. In recent years, neutral glycine has been extensively studied by experimental [23] and theoretical [23(h),24] methods. It is well established that the most stable structure of neutral glycine is **Gly0**, in which both amino hydrogens are in interaction (hydrogen bond) with the carbonyl oxygen. We have optimized this conformer at the MP2/6-31G* level and found a total energy of −283.589804 hartrees. The zero point vibrational energy (ZPVE) at this level is 214 kJ mol^{-1}. The single point total energy at the MP2/LB level is −283.855861 hartrees.

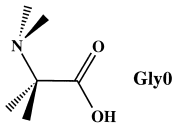

Gly0

In neutral glycine (Gly), there are three basic sites available for protonation: the amino nitrogen atom (N), and the carbonyl (CO) and hydroxyl (OH) oxygen atoms of the carboxyl group. Several quantum calculations [25–35] were performed to determine the proton affinity or the gas phase basicity and/or the relative energy of the various isomers of protonated glycine ($GlyH^+$). They all give the N-protonated form

as the most stable one, in agreement with the well known basicity of primary amines versus carboxylic acids. However, few of these studies considered the energy differences between the three sites of protonation available in glycine. We have therefore undertaken a comprehensive study of the various forms of protonated glycine {N-protonated [$GlyH^+$(N)]; CO-protonated [$GlyH^+$(CO)]; and OH-protonated [$GlyH^+$(OH)]}. As explained in Sec. 2, the search for the most stable conformers of each form of protonated glycine was conducted at two levels of theory: B3LYP/6-31G* and MP2/6-31G*. In general, the geometries obtained with the former method will be discussed only if they are not in agreement with MP2 geometry optimization.

3.1.1. N-protonated glycine

Two conformers of N-protonated glycine were found earlier to be very close together in energy: **1** and **1a** [27,33]. Structure **1** includes in the N–C(H_2)–C=O plane a hydrogen bond (H bond) between the protonating hydrogen and the carbonyl oxygen, whereas in **1a** two weaker interactions occur between the out of plane amino hydrogens and the carbonyl oxygen. Structure **1** is found to be the most stable conformer for N-protonated glycine if the electron correlation correction is taken into account. At the HF level, whatever the basis set used (6-31G*, 6-31G**, 6-31+G**, or 6-311+G**) **1a** is more stable. After correcting for zero-point vibrational energy, the energy difference between both conformations are nearly the same (within 2 kJ mol^{-1}) on either the HF or MP2 PES [27,33]. At the G2(MP2) level conformer **1** is more stable by 2 kJ mol^{-1} than **1a** [30].

The geometry of **1**, optimized at the MP2/6-31G* level is given in Scheme 2. The total energy of **1**, optimized at the MP2/SB level is −283.945602 hartrees; the zero point vibrational energy at this level is 252 kJ mol^{-1} and the single point total energy at the MP2/LB level is −284.204888 hartrees. At the highest level of theory the difference in energy between **Gly0** and **1** is 916 kJ mol^{-1}. Taking into account the zero point vibrational energy of both species leads to an estimation of the proton affinity of neutral glycine of 878 kJ mol^{-1}. This value may be compared with earlier estimations at various levels of theory (see Table 2) and with experimental values.

Proton transfer equilibria between glycine and appropriate reference bases have confined PA(Gly) within 861 and 887 kJ mol^{-1} [20,29,36–39]. This range is in agreement with the proton affinity order [39–41] established from unimolecular dissociation rates of proton-bound heterodimers containing Gly and another amino acid (kinetic method) [42]. The value currently retained in the NIST Standard Reference Database [43] is 886.5 kJ mol^{-1}.

Smith and Radom [44] have shown in many examples that the highly involved G2 method leads to the most accurate theoretical proton affinity values. Their estimates approach true values within chemical accuracy (4–8 kJ mol^{-1}). In agreement with the predictions of Smith and Radom, the G2(MP2) method leads to an estimation of 882 kJ mol^{-1} for PA[Gly(N)] [30], very close to the experimental value (886.5 kJ mol^{-1}). However, the approximation using the MP2/LB level for total energies and MP2/SB for ZPVE corrections, which is less memory and time consuming than G2, leads to a very good approximation of PA[Gly(N)] (878 versus 886 kJ mol^{-1}).

3.1.2. CO-protonated glycine

The conformation of glycine protonated on the carbonyl oxygen was extensively discussed earlier [27,33,34]. First, Jensen [28] proposed six conformers to describe $GlyH^+$(CO). The conformer found to be the most stable at the HF/6-31G* level of theory was **2a**. In this conformer, there is a hydrogen bond between the protonating hydrogen and nitrogen atom. More recently, Zhang and Chung-Phillips confirmed the greatest stability of this conformer [33] at the HF level with various basis sets. However, this HF structure fails to surface from MP2 optimizations [33,34]. The conformer found to be the most stable on the MP2 PES is **2** which, in turn, does not exist on the HF PES.

In this work, **2a** could not be found on the MP2 PES and **2** is found to be the most stable conformer. On the B3LYP PES, both conformers are minima and **2a** is calculated to be more stable than **2** by 48 kJ mol^{-1}. The geometry of **2**, optimized at the MP2/6-

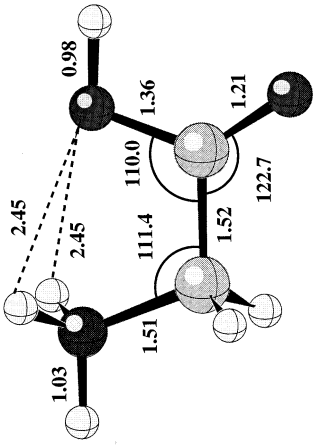

1'

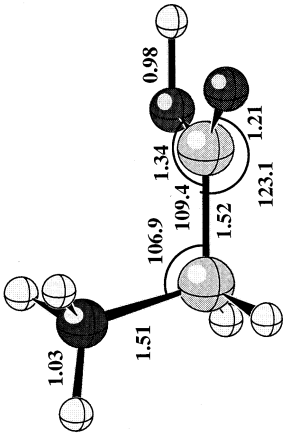

TS 1-1'

Scheme 2.

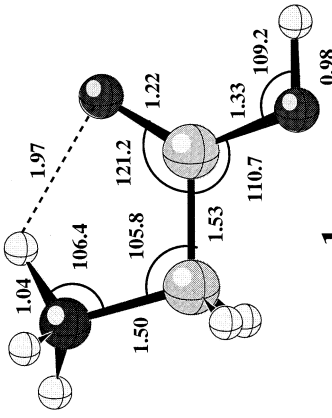

1

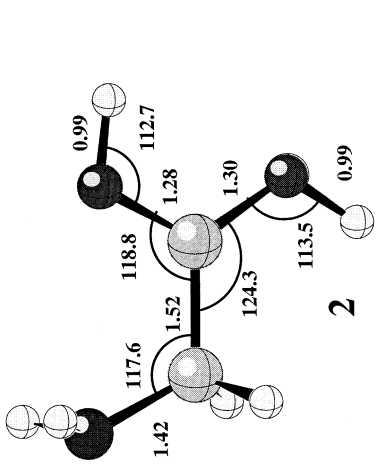

2

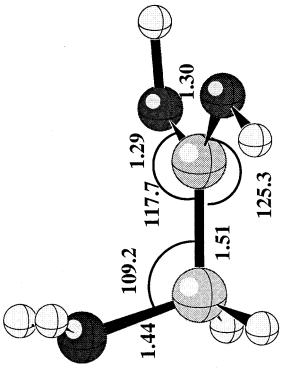

2'

Scheme 3.

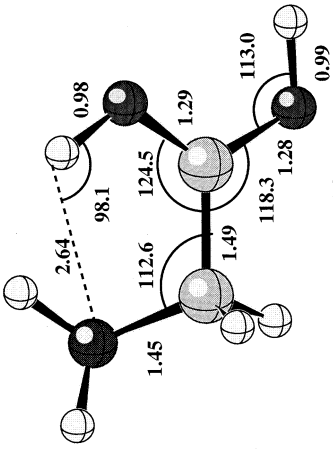

TS 1-2'

Table 2
Proton affinity of glycine calculated at various levels of theory

Level of theory	AP kJ mol^{-1}	Reference
MP2/6-31G*//3-21G	935	[28]
MP2/6-31G*//HF/6-31G*	932	[27]
G2(MP2)	882	[30]
MP2(FC)/6-31+G**//HF/6-31G* +ZPVE(HF/6-31G*)	881	[35]
MP2/6-311+G(2d,2p)//MP2/6-31G*+ZPVE(MP2/6-31G*)	878	this work

31G* level, is given in Scheme 3. The total energy of **2** at the MP2/SB level is −283.891296, the corresponding ZPVE is 245 kJ mol^{-1}, and the improved energy at the MP2/LB level is −284.159612 hartrees. The calculated value of PA[Gly(CO)] is found to be 766 kJ mol^{-1}, i.e. 112 kJ mol^{-1} lower than the PA of the nitrogen atom. This calculated value may be compared with the experimental proton affinity of acetic acid, PA[Aa(CO)] of 784 kJ mol^{-1}, i.e. 18 kJ mol^{-1} higher than our calculated value of PA[Gly(CO)]. This difference may have two origins: an underestimation of PA[Gly(CO)] at the level of theory chosen for its estimation, as seen for PA[Gly(N)], and/or a destabilizing effect of the NH_2 group in beta position of the cation, as shown earlier for acylium ions XCH_2-C^+=O by Lien and Hopkinson [45]. Acetic acid (Aa) as well as its two protonated forms were optimized at the MP2/6-31G* level and improved energies were obtained at the (MP2/LB) level. The corresponding energies are given in Table 3 and lead to PA[Aa(CO)] = 772 kJ mol^{-1} and PA[Aa(OH)] = 756 kJ mol^{-1} (MP2/LB+ZPVE). The difference between the calculated and experimental value of

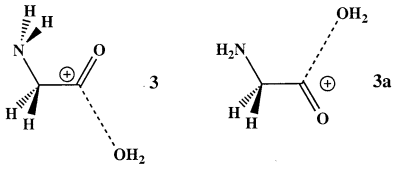

Scheme 3a.

PA[Aa(CO)] is −12 kJ mol^{-1}. This result confirms that the approximation chosen in this work leads to underestimated proton affinities. A very small destabilizing effect of NH_2 on the carbocation is shown by the greater C–C bond length in GlyH(CO) than in AaH(CO) (1.52 versus 1.48 Å).

3.1.3. OH protonated glycine

The protonation on the hydroxyl oxygen leads to a stable ion–dipole complex **3** in which a water molecule is in interaction with an acylium ion [28,31]. This result is confirmed in this work. In the ion–dipole complex $[NH_2\text{-}CH_2\text{-}C(O)\text{–}OH_2]^+$ depicting the OH protonated form, the C(O)–$^+OH_2$ bond is much longer than the C(O)–OH bond in neutral glycine (2.1 [28], 2.35 [31], 2.31 Å (this work) versus 1.36 Å, respectively). The value of the CC=O valence angle is much greater in **3** than in **1** (160.5 ° versus 121.2 °) and prevents the formation of hydrogen bonds between the carbonyl oxygen and the hydrogens of the amine. It is to be noticed that **3a** is not a minimum on the MP2 or B3LYP PES. All starting structures that attempted to describe conformer **3a** collapse, after geometry optimization, onto N-protonated glycine **1′**.

The geometry of **3**, optimized at the MP2/6-31G* level is given in Scheme 4. The MP2/SB total energy

Table 3
Total and relative energies of acetic acid and its two protonated forms at various levels of theory

	PA_{exp}	E(MP2/SB)	E(MP2/LB)	ΔE(SB)	ΔE(LB)	ΔE(LB)+ ZPVE(SB)
Aa	784	−228.410422 ZPVE = 166	−228.622645			
AaH(CO)		−228.714495 ZPVE = 198	−228.928925	798	804	772
AaH(OH)		−228.697616 ZPVE = 183	−228.917133	754	773	756

All energies are in kJ mol^{-1} except for total energies E in hartrees. ΔE is the energy difference between Aa and AaH.

Table 4
Difference in PA between the three protonation sites of Gly (in kJ mol^{-1}) calculated at various levels of theory

Level of theory	AP(Gly(N)) − AP(Gly(CO))	AP(Gly(N)) − AP(Gly(OH))	Reference
B3LYP	120	179	this work
MP2/6-31G*//HF/3-21G	75	180	[28]
MP2/6-31G*//HF/6-31G*	42		[27]
MP2/6-31G**	124	141	[31]
MP2/6-311 + G(3df,2p)//MP2/6311 + G**	122		[33]
MP2/6-311 + G(2d,2p)//MP2/6-31G*	112	122	this work

of **3** is calculated to be −283.879192 hartrees with a zero point vibrational energy equal to 230 kJ mol^{-1}. The improved total energy of **3** is −284.149953 hartrees (MP2/LB). The calculated (MP2/LB+ZPVE) value of PA[Gly(OH)] is found to be 756 kJ mol^{-1}, i.e. 122 kJ mol^{-1} lower than the PA of the nitrogen atom. It is interesting to note that the differences in energy between the OH- and CO-protonated forms of glycine and of acetic acid are 10 and 16 kJ mol^{-1}, respectively. Both values are close to the difference in PA (12 kJ mol^{-1}) between formaldehyde and methanol (PA(formaldehyde = 768 kJ mol^{-1} and PA(methanol) = 756 kJ mol^{-1}) [43]). In the carboxyl group, the presence of OH has little influence on the PA of the carbonyl oxygen and vice versa.

Table 4 summarizes the difference in PA between the basic sites of glycine calculated earlier and in this work at various levels of theory.

3.2. Decomposition mechanisms of protonated glycine

Protonated glycine has been produced in the gas phase by a variety of ionization methods including chemical ionization (CI) [1,2,4,9,13], secondary ion mass spectrometry [5,6], laser desorption (LD) [7], fast atom bombardment (FAB) [10,13,14], plasma desorption (PD) [11], and electrospray ionization [15,16].

The source decompositions of $GlyH^+$ formed by these techniques (examples: CI (H_2 and CH_4 [4]; LD [7]; FAB [10]; PD [11]) or the decompositions induced by collision induced dissociation (CID) of low [14–16] or high [10,13] energy lead to prominent formation of the immonium ion **I** = $[NH_2CH_2]^+$ at *m/z* 30. After total exchange of the acidic hydrogens the immonium ion is shifted at *m/z* 32 [13,16]. In the high energy CID spectra of $[NH_2CD_2COOH]H^+$ and $[ND_2CD_2COOD]D^+$ ions, the immonium ion appears at *m/z* 32 and *m/z* 34, respectively [13]. These results reveal that the hydrogens involved in the neutral loss of 46 u are exchangeable hydrogens, i.e. the hydroxylic hydrogen and one of the hydrogens of the protonated amine. The easy formation of this ion was confirmed quantitatively for $GlyH^+$ by Kebarle et al. [15]. These authors have determined the formation threshold for each of the fragment ions of energized $GlyH^+$, showing $NH_2CH_2^+$ to be the fragment of smallest critical energy: 184 kJ mol^{-1}.

We have seen in the Introduction that the elemental composition associated with this loss of 46 u is [C, H_2, O_2]. Four different processes may lead to the elimination of [C, H_2, O_2] (Scheme 1): (1) elimination of formic acid (HCOOH) from the N-protonated form of glycine, (2) consecutive losses of carbon dioxide (CO_2) and dihydrogen (H_2) from $GlyH^+$(N); (3) elimination of dihydroxycarbene [$C(OH)_2$] from $GlyH^+$(CO); and (4) successive losses of water (H_2O) and carbon monoxide (CO) from $GlyH^+$(OH). Table 1 shows that three among these processes lead to final states, very close together in energy: **A** = **I** + HCOOH; **B2** = **I** + CO_2 + H_2; **D2** = **I** + H_2O + CO. The relative energies (ΔE) calculated at the highest level of theory are 125, 86, and 129 kJ mol^{-1} above **1**, respectively. The final state **C** = **I** + $C(OH)_2$ associated with loss of dihydroxycarbene is much higher in energy (ΔE = 313 kJ mol^{-1}).

To better understand the thermochemical constraints associated with each method of fragmenta-

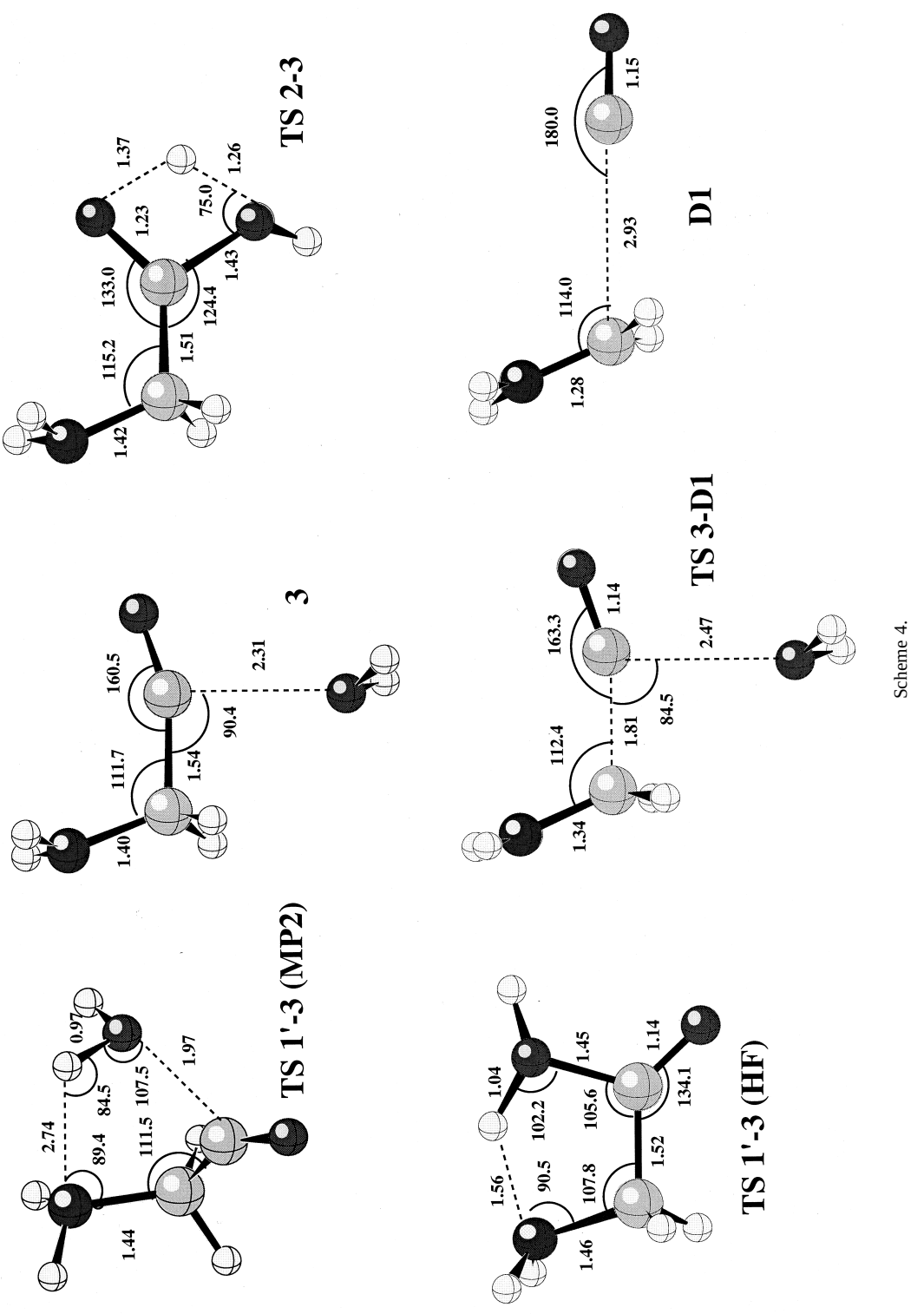
TS 2-3
1.37
1.26
75.0
1.23
133.0
1.43
124.4
115.2
1.51
1.42
D1
180.0
1.15
2.93
114.0
1.28
3
160.5
2.31
90.4
111.7
1.54
1.40
TS 3-D1
163.3
1.14
2.47
84.5
112.4
1.81
1.34
TS 1'-3 (MP2)
2.74
0.97
89.4
84.5
107.5
1.97
111.5
1.44
TS 1'-3 (HF)
1.04
1.45
1.14
102.2
105.6
134.1
1.56
90.5
107.8
1.52
1.46

Scheme 4.

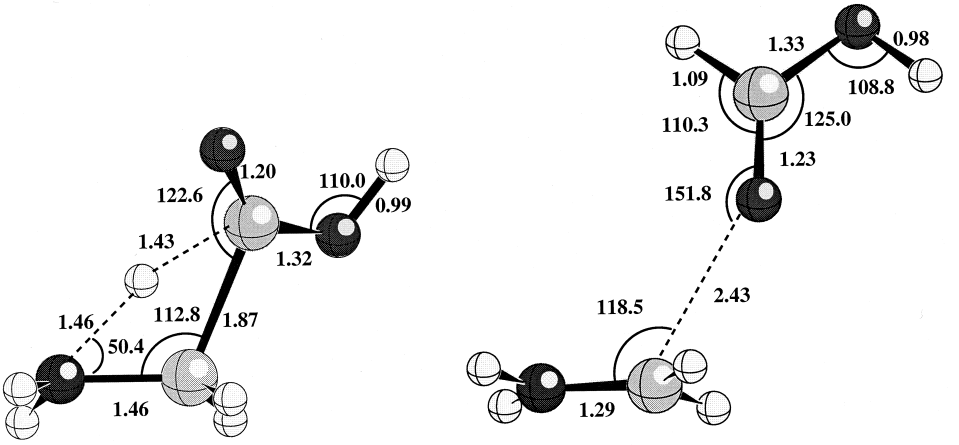

Scheme 5.

tion, we have calculated the detailed pathway of each fragmentation at the same levels as previously.

3.2.1. Process A: Loss of HCOOH

The best precursor for the loss of formic acid is the N-protonated form of glycine. To take into account the involvement of two labile hydrogens in the loss of 46 u the migration of one hydrogen from the protonated amine to the carboxyl carbon is required. The transition state (**TS 1-4**) linking $GlyH^+$(N) **1** to the intermediate ion–dipole complex between immonium and formic acid **4** is located 378 kJ mol^{-1} higher in energy than **1**. This very high energy is explained by an unfavorable 1,3 H migration requiring a very tight four center transition state. The main differences between the geometries of **TS 1-4** optimized at the MP2/6-31G* (given in Scheme 5) and B3LYP/6-31G* levels are the bond lengths between: the migrating hydrogen and NH_2 $d(H_{mig}\text{-}NH_2)$; the migrating hydrogen and the carbon of the carboxylic group $d[H_{mig}\text{-}C(OOH)]$; CH_2 and the carbon of the carboxylic function $d[CH_2\text{-}C(OOH)]$ [1.46, 1.43, and 1.87 Å (MP2) versus 1.43, 1.47, and 1.93 Å (B3LYP), respectively]. The geometry of this transition state is characterized by a great increase in $d(CH_2\text{-}C(OOH)$ relative to the corresponding distance in $GlyH^+$(N), prior to the dissociation. In this state the migrating hydrogen is shared by the nitrogen and the carboxyl carbon.

The intermediate **4** is a stable species lying 72 kJ mol higher in energy than **1**. The main differences in geometry between MP2 (Scheme 5) and B3LYP optimizations are the distance between CH_2 and the carbonyl oxygen {2.43 (MP2) versus 2.25 Å (B3LYP) and the angle between CH_2, the carbonyl oxygen, and the carbon of the preformed formic acid [151.8 ° (MP2) versus 132.8 ° (B3LYP)]}.

The final state **A** at 125 kJ mol^{-1} above **1** is reached after cleavage of the CH_2–O=C(H)OH bond, which requires 53 kJ mol^{-1}. In summary, the different steps associated with **1** losing formic acid are

$$\mathbf{1}(0) \rightarrow \mathbf{TS\ 1\text{-}4}\ (378) \rightarrow \mathbf{4}\ (72)$$
$$\rightarrow \mathbf{A} = \mathbf{I} + \mathrm{HCOOH}\ (125)$$

3.2.2. Process B: Consecutive losses of CO_2 and H_2

The consecutive losses of CO_2 and H_2 involve two different reactions: $GlyH^+ \rightarrow CH_3NH_3^+ + CO_2$ and $CH_3NH_3^+ + CO_2 \rightarrow CH_2NH_2^+ + CO_2 + H_2$.

3.2.2.1. Loss of carbon dioxide. The best precursor for the loss of carbon dioxide is $GlyH^+$(N). The atom involved in the rearrangement of $GlyH^+$ (N) into the

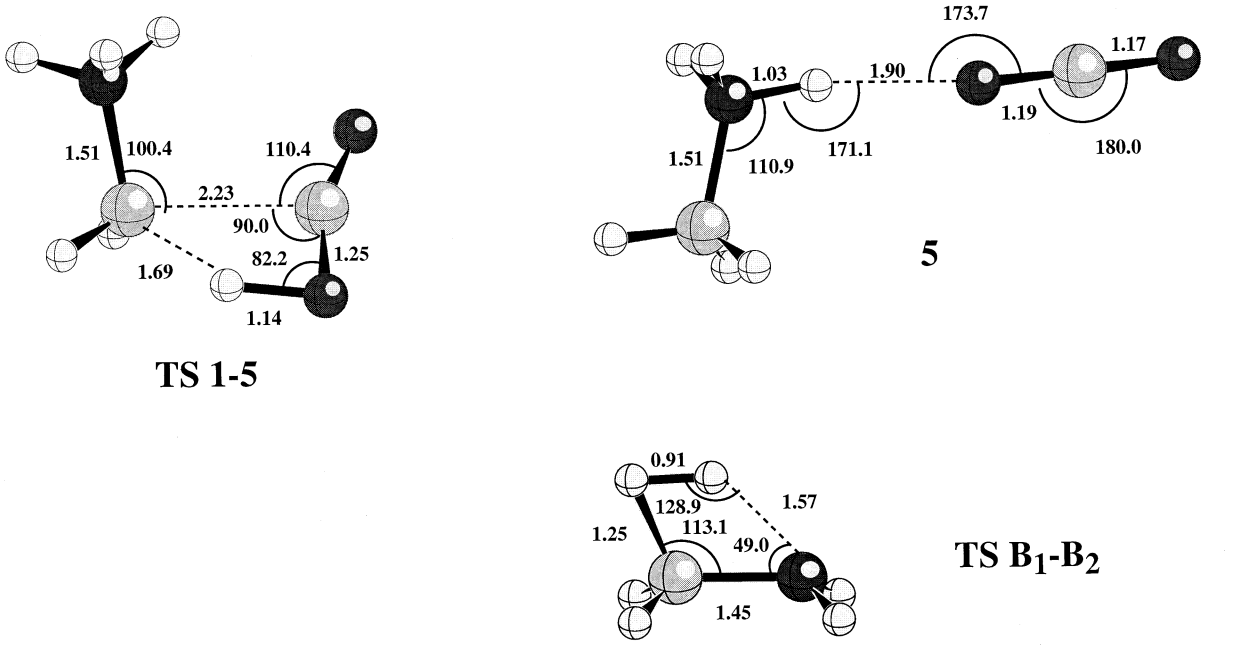

Scheme 6.

ion–molecule complex $[O{=}C{=}O\cdots HNH_2CH_3]^+$ **5** is the hydroxyl hydrogen. The 1,3 H transfer involves a four center transition state **TS 1-5** (Scheme 6). A high relative critical energy is found at 305 kJ mol^{-1}. This transition state is characterized by an important stretch of the C–C bond [2.23 Å versus 1.53 Å in $GlyH^+(N)$] and a very small increase of the O–H bond linking the hydroxyl oxygen and the migrating hydrogen. The intermediate state $[O{=}C{=}O\cdots HNH_2CH_3]^+$ **5** is a very stable ion–dipole complex located −81 kJ mol^{-1} relative to **1**. The great stability of this species may be due to the intrinsic stability of both components and to the interaction between one oxygen of the carbon dioxide and one hydrogen bearing a part of the charge of the protonated nitrogen. Globally, the transition state more closely resembles **1** than the $[CO_2$-$NH_3CH_3]^+$ complex. Only small differences appear between the MP2 and B3LYP geometries of **TS 1-5** and **5**: the length of the C–C bond is 2.23 Å (MP2) versus 2.27 Å (B3LYP) in **TS 1-5**; the interatomic distance $(O)C{=}O\cdots HN(H_2)$ is 1.90 Å (MP2) versus 1.86 Å (B3LYP) in **5**.

The separation of fragments forming **5** leads to protonated methylamine and carbon dioxide identified as the final state **B1** in Table 1. **B1** is −44 kJ mol^{-1} more stable than **1**. The dissociation energy of $(O)C{=}O\cdots HN^+(H_2)$ bond in **5** is calculated to be 37 kJ mol^{-1}.

3.2.2.2. Loss of dihydrogen. The fragmentation following the loss of CO_2 to give the immonium is a 1–2 elimination of H_2 from protonated methylamine. This loss of H_2 is a four center elimination with a great energy demand. The transition state associated with this elimination is calculated to lie 342 kJ mol^{-1} higher in energy than **B1**, i.e. 298 kJ mol^{-1} above **1**. The MP2 geometry of this transition state (**TS B1-B2**) is given in Scheme 6. In the transition state, the leaving hydrogen, H_N (initially borne by the nitrogen) is further away from the nitrogen atom than the leaving hydrogen, H_C, from the carbon atom [$d(H_N - NH_2) = 1.57$ Å versus $d(H_C - CH_2) = 1.25$ Å. Moreover, the H_N–H_C bond is preformed in the transition state [$d(H_N - H_C) = 0.91$ Å]. MP2 and B3LYP geometries of **TS B1-B2** are very similar.

The final state **B2** associated with this elimination

(**B2** = **I** + CO_2 + H_2) lies 86 kJ mol^{-1} higher in energy than **1**. The different steps associated with process B are summarized as follow:

1(0) → **TS 1-5** (305) → **5** (−81) → **B1** (−44)

→ **TS B1-B2** (298)

→ **B2** = **I** + CO_2 + H_2 (86)

3.2.3. Process C: Loss of $C(OH)_2$

The precursor for a direct loss of $C(OH)_2$ is the CO-protonated form of glycine **2** (or **2′**). Starting from **1** the isomerization requires transfer of the protonating hydrogen to the oxygen of the carbonyl group. This transfer was studied earlier by Zhang et al. [33]. Irrespective of the basis set used, they found two different types of transition states depending on the level of calculation (HF versus MP2). Without electron correlation the transition state is a molecular complex containing a strained five-membered ring structure -H_{mig}-$N(H_2)$-$C(H_2)$-C(OH)-O- where H_{mig} is the migrating proton. This transition state connects **1** and **2a** (see above). With electron correlation we have seen before that **2a** is not a minimum on the PES of $GlyH^+$. The MP2 transition state connects **1** to a conformer **2′** in which the plane containing the nitrogen atom and both carbon atoms is perpendicular to the one containing $C(OH)_2$. The MP2 geometries of **2′** and of **TS 1-2′** that we have optimized are given in Scheme 3. To reach the transition state **TS 1-2′**, **2** undergoes rotation about the C–C bond to approach the oxygen bearing the migrating hydrogen near the nitrogen and rotation about C–N to move the amino hydrogens away from the migrating hydrogen and make room for this later. This transition state is very hard to localize because the proton in the CO-protonated form of glycine undergoes easy migration to the nitrogen atom, an extremely favorable process. This may be attributed to the great differences in PA between the carbonyl oxygen and the nitrogen. A rotation around C–C in **2′** leads to the MP2 most stable form, i.e. **2**. **TS 1-2′**, **2′**, and **2** are located 133, 118, and 112 kJ mol^{-1} higher in energy than **1**, respectively.

Using the B3LYP density functional we found two geometries to describe the transition state. One very similar to the HF geometry optimized by Zhang et al. [33] connects **1** to **2a** and is located 72 kJ mol^{-1} above **1**. The other one, with the same geometrical parameters as the MP2 **TS 1-2′**, connects **1** to **2′** and is located 150 kJ mol^{-1} above **1**.

The last step of the fragmentation is a simple C–C bond breaking leading to the dihydroxycarbene and the immonium ion (state **C**). This **C** state is 313 kJ mol^{-1} higher in energy than **1**. The dissociation energy required to break the C–C bond from conformer **2** is calculated to be 201 kJ mol^{-1}. In this process, the rate limiting step is the high C–C dissociation energy in **2**. In summary:

1(0) → **TS 1-2′** (133) → **2′** (118) → **2** (112)

→ **C** = **I** + $C(OH)_2$ (313)

3.2.4. Process D: Consecutive losses of H_2O, CO

The best precursor for an initial loss of water is the glycine protonated on the hydroxyl oxygen, **3**. We have seen before that for such a structure, ab initio calculations [28,31,this work] reveal the formation of an ion–dipole complex $[NH_2\text{-}CH_2\text{-}C(O)\text{–}OH_2]^+$ preceding an impending loss of water that can then be followed by CO elimination. From **1**, two pathways may lead to consecutive losses of H_2O and CO. The first one requires four steps: (1) rotation of the C–C bond to bring the hydroxyl oxygen close to the hydrogens of the protonated amine (conformer **1′** in Scheme 2); (2) proton transfer from N to OH giving **3**; (3) cleavage of the C(O)–$^+OH_2$ bond; and (4) cleavage of the $NH_2CH_2^+$–C=O bond. The second one, also in four steps, starts with the isomerization of the N- to the CO-protonated form (**1** → **2**, see process C above). A second isomerization leads from **2** to **3**. The last two steps are the same as in the first pathway.

3.2.4.1. First pathway. The transition state associated with the rotation **1** → **1′** (**TS 1-1′**) and the conformer **1′** are located 32 and 18 kJ mol^{-1} above **1**, respectively. In the transition state the NCC plane is perpendicular to the one containing the carboxyl group. In conformer **1′**, the nitrogen and the hydroxyl oxy-

gen are vis à vis. The MP2 geometries of **TS 1-1′** and **1′** are given in Scheme 2. No significant difference is obtained by B3LYP optimization.

As for **TS 1-2′**, the transition state **TS 1′-3** is difficult to localize because the proton in the OH-protonated form of glycine undergoes easy migration to the nitrogen atom. We have seen before that structure **3a** is not a minimum on the MP2 or B3LYP PES of $GlyH^+$. In fact **TS 1′-3** very much resembles **3a** or, in other words, **3a** is a transition state. This transition structure (see Scheme 4) lies 153 kJ mol^{-1} higher in energy than **1** and 31 kJ mol^{-1} higher than **3**. For the same reaction Uggerud located the transition state 147 kJ mol^{-1} higher than **1** and only 6 kJ mol^{-1} higher than **3** [31]. The B3LYP and MP2 geometries of **TS 1′-3** are very similar. However, because HF and MP2 calculations were shown [33] to give very different geometries for the transition state associated with the isomerization $GlyH^+(N) \rightarrow GlyH^+(CO)$ we have optimized at the HF/6-311+G(2d,2p) level the transition state associated with the isomerization GlyH(N) → GlyH(OH). The corresponding geometry is given in Scheme 4. With electron correlation the transition state is a $[NH_2CH_2C^+O, H_2O]$ molecular complex containing a five-membered ring structure -H_{mig}-$N(H_2)$-$C(H_2)$-C(O)-O(H)- where H_{mig} is the migrating proton and in which $d(H_{mig}\text{-}N)$ = 2.74 Å and $d(OC\text{-}OH_2$ = 1.97 Å). HF optimization of **TS 1′-3** with a large basis set dramatically increases the bonding interactions between both the proton and nitrogen as well as the carbonyl carbon and water oxygen [$d(H_{mig}\text{-}N)$ = 1.56 Å and d[OC-OH_2 = 1.45 Å)]. We used both geometries (MP2/SB and HF/LB) to calculate final energies at the MP2/LB level including the ZPVE obtained for each optimization level. The corresponding relative energies are 153 (MP2) and 145 (HF) kJ mol^{-1}. Given the great difference between both geometries and their small difference in energy, the MP2/LB PES describing the proton transfer between the nitrogen and the hydroxyl oxygen atoms is expected to be very flat.

In the ion–dipole complex $[NH_2\text{-}CH_2\text{-}C(O)\text{–}OH_2]^+$ depicting the OH protonated form, we have seen that the C(O)–$^+OH_2$ bond is much longer than the C(O)–OH bond in neutral glycine. Consequently, the activation energy (E_a) associated with the breaking of this bond is expected to be very low. The transition state **TS 3-D1** and the fragments $NH_2\text{-}CH_2\text{-}C^+{=}O$ and H_2O (state **D1** in Table 1) (see Scheme 4) are located 127 and 112 kJ mol^{-1} higher in energy than **1**, respectively. The C(O)–$^+OH_2$ bond breaking requires an E_a = 5 kJ mol^{-1}. However, the difference in energy between **3** and **D1** (−10 kJ mol^{-1}) could be surprising. This difference would indicate that the decoordination of H_2O is exothermic. In fact the difference in energy between **3** and **D1** is calculated to be +12 and 0 kJ mol^{-1} at the MP2/SB and MP2/SB+ZPVE levels. The inversion in stability arises from the single point calculation at the MP2/LB+ZPVE(SB) level. The MP2/LB PES describing the cleavage of the $C(O)^+$–OH_2 bond is very flat and the single point approximation fails.

The last step of the fragmentation is the loss of CO from a $H_2NCH_2C^+{=}O$ ion experimentally not observed. It is generally admitted that direct elimination of two neutral species (here H_2O and CO) without detecting any intermediate ion means that the latter is produced near or above its dissociation limit, or that it is not a stable species. The enthalpy of reaction 1:

$$H_2NCH_2C^+{=}O \rightarrow NH_2CH_2^+ + CO \quad (1)$$

was first estimated to be −6 kJ mol^{-1} by Tsang and Harrison [4]. It was later calculated (MP2/6-31G**//HF/6-31G*) to be −53 kJ mol^{-1} [45]. More recently, studies by van Dongen et al. [46] revealed that the $H_2NCH_2C^+{=}O$ ion should be considered an electrostatically bound ion/molecule complex $[H_2NCH_2\text{–}CO]^+$. Finally, recent calculations by Uggerud [31] at the MP2/6-31G** level determined that the dissociation of $[H_2NCH_2\text{–}CO]^+$ into $[NH_2CH_2]^+$ and CO requires 19 kJ mol^{-1}. In this work, we confirm that the $H_2NCH_2C^+{=}O$ ion is an electrostatically bound ion/molecule complex because the distance between the methylene group and the carbon of the carbon monoxide is calculated (MP2) to be 2.93 Å. The final state associated with the successive losses of H_2O and CO giving the immonium ion (state **D2** in Table 1) lies 129 kJ mol^{-1} above **1**. In other words, the

decomplexation of CO requires 17 kJ mol^{-1}. The PES associated with consecutive losses of H_2O and CO via pathway 1 is summarized as follows:

1(0) → **TS 1-1′** (32) → **1′** (18) → **TS 1′-3** (153)

→ **3** (122) → **TS 3-D1** (127) → **D1** (112)

→ **D2** = **I** + H_2O + CO (129)

Because (1) the rate limiting step in the fragmentation is the transition state **1′** → **3** located 31 kJ mol^{-1} higher than **3** and (2) **3**, **TS 3-D1**, **D1**, and **D2** are very close together in energy (within 17 kJ mol^{-1}), it is easy to understand why the loss of H_2O is not observed: all the ions of structure **1′** having enough internal energy to isomerize into **3** have enough energy to decompose into **D2** = **I** + H_2O + CO. The minimum energy required for this fragmentation, 153 kJ mol^{-1}, is in reasonable agreement with the experimental appearance threshold of $CH_2NH_2^+$ that is given as 184 ± 8 kJ mol^{-1} [15].

3.2.4.2. Second pathway. The first step of this second pathway is the isomerization **1** → **2** that requires an activation energy of 133 kJ mol^{-1} (see above).

The second step is the isomerization **2** → **3**. The 1,3 H migration via a very tight four center transition state is expected to require a great activation energy even if the PA of both oxygens are very close to one another. The geometry of **TS 2-3** is characterized by a protonating hydrogen in interaction with both oxygen atoms [d(HO–H^+ = 1.26 Å versus d(C=O–H^+) = 1.37 Å). The structure of **TS 2-3** better resembles **2** than **3** (see Scheme 4). This transition state is located 302 kJ mol^{-1} above **1**. The third and fourth steps have already been described above. In summary:

1(0) → **TS 1-2′** (133) → **2** (112) → **TS 2-3** (302)

→ **3** (122) → **TS 3-D1** (127) → **D1** (112)

→ **D2** = **I** + H_2O + CO (129)

The minimum energy required for consecutive losses of H_2O + CO via isomer **2** is 302 kJ mol^{-1}. This pathway may be excluded because the energy demand for the same fragmentation is much lower via isomer **3** (153 kJ mol^{-1}, vide supra).

3.2.5. Reactions in competition with the loss of 46 u

3.2.5.1. Loss of CO. In addition to the loss of 46 u, the low energy CID spectrum of $GlyH^+$ shows a minor loss of CO [15,16]. This fragmentation had been previously observed in the metastable ion spectrum of FAB- or CI-generated $GlyH^+$ [10,13]. This unimolecular decomposition is accompanied by a substantial release of kinetic energy ($T_{0.5}$ = 0.46 eV), indicating that CO loss is accompanied by molecular reorganization. This is consistent with the above picture because the initially formed ion–dipole complex $[NH_2CH_2C(O)–OH_2]^+$ **3** may easily rearrange to a $[H_2O–NH_2CH_2–CO]^+$ form **6**. Structure **6** is better described as a loosely bound complex between the H_2O-immonium ionic species and carbon monoxide because CO is far (3.03 Å) from CH_2, its initial anchoring site, whereas H_2O is close (1.69 Å) to one hydrogen of NH_2. The transition state **TS 3-6** is an acylium ion in which the water oxygen interacts with both a hydrogen of the amine and the carbonyl carbon [d(H_2O–C=O=2.71 Å; d(H_2O–H(NH) = 2.25 Å). The geometries of **6** and **TS 3-6** are given in Scheme 7. Similar B3LYP geometries were optimized. The activation energy required for the isomerization **3** → **6** is 125 kJ mol^{-1} above **1**, i.e. 3 kJ mol^{-1} above **3** and 85 kJ mol^{-1} above **6**, which is a very stable species (40 kJ mol^{-1} higher in energy than **1**). A barrier of 172 kJ mol^{-1} was given earlier by Uggerud [31]. The bond dissociation energy associated with the C–C(=O) bond breaking is 35 kJ mol^{-1} and leads to state **E** (Table 1) [**E** = (H_2O–$NH_2CH_2^+$ + CO] 75 kJ mol^{-1} above **1**.

Loss of CO may be followed by loss of water to lead to the final state **D2**. However, given the great energy released during the fragmentation **3** → **D1**, it is likely that a great part of $[MH\text{-}CO]^+$ ions do not have enough internal energy to lose H_2O. The energy profile for the consecutive losses of CO and H_2O may be summarized as follows:

1(0) → **TS 1-1′** (32) → **1′** (18) → **TS 1′-3** (153)

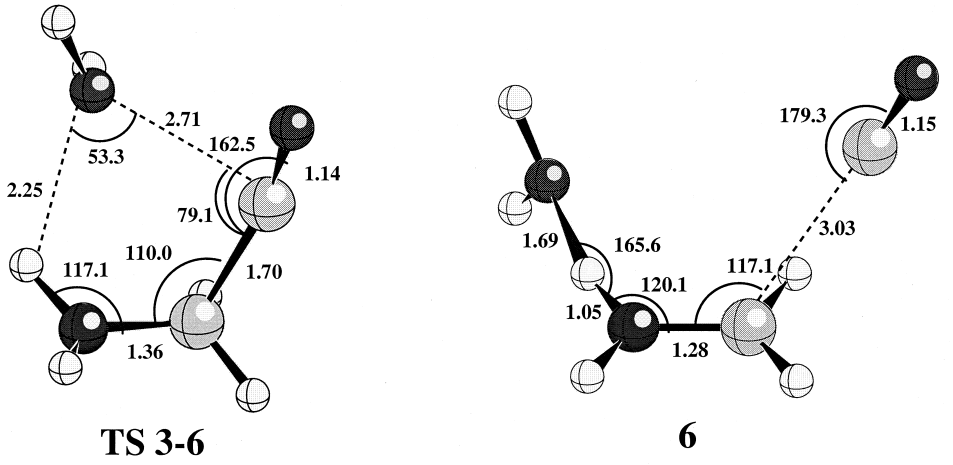

Scheme 7.

→ **3** (122) → **TS 3-6** (125) → **6** (40)

→ **E** (75) → **D2** = **I** + H_2O + CO (129)

Initial loss of CO or H_2O involves the same determining step that is the transition state associated with the isomerization **1** → **3**. The potential energy surface appears to be such that either loss of H_2O or CO (or both) may easily occur, depending on the experimental conditions.

3.2.5.2. Loss of NH_3. Loss of ammonia is a common fragmentation of α-amino acids and especially for asparagine, glutamine, cysteine, methionine, tyrosine, thryptophan, and lysine but has never been observed in the spectra of glycine. Recently [16] this fragmentation was shown to start with an elongation of the C–NH_3^+ bond. This elongation is assisted by a cyclisation involving the lateral chain and stabilizing the incoming carbocation. In the case of glycine there is no lateral chain and the loss of NH_3 leads to a primary carbocation destabilized by the carboxyl group. From **1** the energy needed to break the C–NH_3^+ bond is calculated to be 326 kJ mol^{-1}.

4. Discussion

The six fragmentations of N-protonated glycine **1** described above are:

$$\mathbf{1} \rightarrow \mathbf{A} = [NH_2CH_2]^+ + HCOOH \quad (378\ kJ\ mol^{-1}) \quad (1)$$

$$\mathbf{1} \rightarrow \mathbf{B2} = [NH_2CH_2]^+ + CO_2 + H_2 \quad (305\ kJ\ mol^{-1}) \quad (2)$$

$$\mathbf{1} \rightarrow \mathbf{C} = [NH_2CH_2]^+ + C(OH)_2 \quad (313\ kJ\ mol^{-1}) \quad (3)$$

$$\mathbf{1} \rightarrow \mathbf{D2} = [NH_2CH_2]^+ + H_2O + CO \quad (153\ kJ\ mol^{-1}) \quad (4)$$

$$\mathbf{1} \rightarrow \mathbf{E} = [H_2O\text{-}HNHCH_2]^+ + CO \quad (153\ kJ\ mol^{-1}) \quad (5)$$

$$\mathbf{1} \rightarrow \mathbf{F} = [CH_2COOH]^+ + NH_3 \quad (326\ kJ\ mol^{-1}) \quad (6)$$

In parentheses are given the critical energies associated with each fragmentation. The critical energy is

defined here as the minimum energy needed to observe the fragmentation. Among these fragmentations, (1), (2), (3), and (6) have critical energies higher than 300 kJ mol^{-1} whereas (4) and (5) have the same critical energy of 153 kJ mol^{-1}.

For molecular ions having low internal energies only (4) and (5) may be in competition. However, we have seen before that loss of CO may be observed only for molecular ions with long lifetimes. $[GlyH\text{-}CO]^+$ ions are observed in significant abundance only in the metastable ion spectra [10,13] whereas they appear in low abundance in the low energy CID spectra of $GlyH^+$ [15,16]. That is to say that the "low energy" collisions occuring in the triple quadrupole lead to protonated glycines having relatively short lifetimes, i.e. too much internal energy to rearrange into **6**.

For ions with high internal energy (higher than 300 kJ mol^{-1}) we may ask: Are reactions (1), (2), (3), and (6) in competition with (4) and (5)? Experimentally, Wesdemiotis et al., in a very comprehensive study, have studied the neutral fragment reionization (N_fR) mass spectra of $GlyH^+$ [13]. The neutral species liberated upon high energy CID are reionized. High energy collisions and reionization are known as highly energetic reactions. The mixture of ions obtained upon reionization are: $[H_2O]^{\cdot+}$, $[CO]^{\cdot+}$, $[CH_2NH_3]^{\cdot+}$, $[CO_2]^{\cdot+}$, $[COOH]^+$, and $[CH_2O_2]^{\cdot+}$. Among these ions, which may be those related to loss of 46 u occurring under CID conditions? In the first approximation: $[H_2O]^{\cdot+}$ and $[CO]^{\cdot+}$ [reaction (4)]; $[CH_2O_2]^{\cdot+}$ [reaction (1) and/or (3)], and $[CO_2]^{\cdot+}$ [reaction (2)].

The formation of $[H_2O]^{\cdot+}$ and $[CO]^{\cdot+}$ after losses of H_2O and CO from $GlyH^+$ is very likely because the mechanism associated with these fragmentations was demonstrated to be energetically and kinetically very favourable at low energy.

The observation, upon reionization, of radical cations at *m/z* 46 implies the loss of either HCOOH or $C(OH)_2$ under collision. One energetic argument allows us to eliminate the loss of HCOOH. Loss of NH_3 was never observed in the direct, metastable, or CID mass spectra of $GlyH^+$. The critical energy associated with this loss of NH_3 by a simple bond cleavage, E_a (6) (326 kJ mol^{-1}), is calculated to be lower than that associated with loss of HCOOH, E_a (1) (378 kJ mol^{-1}). Moreover, the elimination of the latter involves a time demanding rearrangement. Because $[GlyH\text{-}NH_3]^+$ is not observed, the elimination of HCOOH is very unlikely. Consequently, only $C(OH)_2$ may be the precursor of the radical cation at *m/z* 46 because the critical energy associated with its formation by simple bond cleavage, E_a (3) (313 kJ mol^{-1}), is lower than E_a (6).

In first approximation, the presence of $[CO_2]^{\cdot+}$ in the N_fR mass spectrum of $GlyH^+$ could indicate that reaction (2) occurs under CID conditions and that $[H_2]^{\cdot+}$ is not observed because of its high ionization energy (15.42 eV compared to 12.6, 14.0, 9.0, 13.8, and 11.3 eV for H_2O, CO, CH_3NH_2, CO_2, and HCOOH, respectively [43] and about 8 eV for $^{\cdot}COOH$ [47,48]. However, energetic and kinetic arguments converge to exclude this process from the fragmentation of $GlyH^+$. Protonated methylamine (*m/z* 32), the ionic species correlated with the elimination of CO_2, is never observed in the mass spectra of protonated glycine. On energetic grounds, the direct elimination of CO_2 and H_2 without detecting any $[CH_3\text{-}NH_3]^+$ intermediate ion requires that the rate limiting step in the fragmentation be the initial barrier associated with **TS 1** → **5**. In the present case, **TS 1** → **5** located 305 kJ mol^{-1} above **1** is the limiting step but the relative energies of **5**, **B1**, **TS B1** → **B2**, and **B2** are −81, −44, 298, and 86 kJ mol^{-1}, respectively, relative to **1**. The dramatic energy difference between **TS 1** → **5** and the very stable species **5** and **B1** suggests that CO_2 loss is accompanied by a great energy release. Consequently, protonated methylamine would be observed because the $[MH\text{-}CO_2]^+$ ions do not have enough energy to fragment. The absence of $[CH_3\text{-}NH_3]^+$ ions in the mass spectra leads us to conclude that **1** → **5** does not occur. However, **TS 1** → **5** is close in energy to the final state **C** demonstrated previously to be formed at high energy. This may be due to the fact that **C** arises from an easy proton transfer from **1** to **2** and a simple bond cleavage in **2**, whereas formation of **5** requires a highly constrained, kinetically unfavourable transition state.

As proposed earlier by Wesdemiotis [13], the origin of $[CO_2]^{\cdot +}$ in the N_fR mass spectrum of $GlyH^+$ is probably ^+COOH because the neutralization–reionization mass spectrum of the carboxyl cation is dominated by the fragment ion *m/z* 44 ($[CO_2]^{\cdot +}$) [47]. The ^+COOH ion (in the N_fR mass spectrum of $GlyH^+$) proceeds either from heterolytic cleavage of neutralized GlyH to form ^+COOH and $NH_3CH_2^+$ after reionization or from decomposition of $[C(OH)_2]^{\cdot +}$ [49].

The last point of this discussion concerns the comparison between the critical energies of each fragmentation evaluated at different levels of theory. In general, the B3LYP/6-31G*, MP2/6-31G*, or MP2/6-311+G(2d,2p)//MP2/6-31G* calculations without ZPVE corrections lead to relative energies greater in absolute value than MP2/6-311+G(2d,2p)//MP2/6-31G*+ZPVE values, but yield the correct order of stability. Often, relative energies obtained at B3LYP/6-31G* and MP2/6-311+G(2d,2p)//MP2/6-31G* levels without ZPVE corrections are very close together. The greatest differences are observed for species involving long range ion–dipole interactions and in particular for **TS 1** $\rightarrow$ **2′** and **TS 1′** $\rightarrow$ **3**. It may be that DFT is not as reliable for determining transitions states as it is for minima.

5. Conclusion

At low energy, fragmentation of $GlyH^+$ by loss of 46 u requires proton transfer from the amino to the hydroxyl group. This yields an ion–molecule intermediate that can either eliminate H_2O + CO or CO, depending upon the lifetime of the intermediate, which is determined by the specific experimental conditions. In any case, fragmentation of the OH-protonated isomer is the only low energy process.

At higher energy, there appears a new elimination mechanism of 46 u: direct loss of dihydroxycarbene. This fragmentation first requires proton transfer from the nitrogen to the carbonyl oxygen. Elimination of formic acid is ruled out by the present calculations. In general, all the processes involving a 1,3 H hydrogen transfert via a tight four center transition state are energetically unfavourable.

References

[1] G.W. Milne, T. Axenrod, H.M. Fales, J. Am. Chem. Soc. 92 (1970) 5170.
[2] P.A. Leclerq, D.M. Desiderio, Org. Mass Spectrom. 7 (1973) 515.
[3] M. Meot-Ner, F.H. Field, J. Am. Chem. Soc. 95 (1973) 7207.
[4] C.W. Tsang, A.G. Harrison, J. Am. Chem. Soc. 98 (1976) 1301.
[5] A. Benninghoven, W.K. Sichtermann, Anal. Chem. 50 (1978) 1180.
[6] T.P. Fan, E.D. Hardin, M.L. Vestal, Anal. Chem. 56 (1984) 1870.
[7] C.D. Parker, D.H. Hercules, Anal. Chem. 57 (1985) 698.
[8] C.D. Parker, D.H. Hercules, Anal. Chem. 58 (1986) 25.
[9] M. Vairamani, R. Srinivas, G.K. Viswanadharao, Indian J. Chem. 27B (1988) 264.
[10] W. Kulik, W. Heerma, Biomed. Mass Spectrom. 15 (1988) 419.
[11] S. Bouchonnet, J.P. Denhez, Y. Hoppilliard, C. Mauriac, Anal. Chem. 64 (1992) 743.
[12] G. Bouchoux, S. Bourcier, Y. Hoppilliard, C. Mauriac, Org. Mass Spectrom. 28 (1993) 1064.
[13] S. Beranova, J. Cai, C. Wesdemiotis, J. Am. Chem. Soc. 117 (1995) 9492.
[14] N.N. Dookeran, T. Yalcin, A.G. Harrison, J. Mass Spectrom. 31 (1996) 500.
[15] J.S. Klassen, P. Kebarle, J. Am. Chem. Soc. 119 (1997) 6552.
[16] F. Rogalewicz, Y. Hoppilliard, G. Ohanessian, Int. J. Mass Spectrom., 195/196, 565 (2000).
[17] M.J. Frisch, G.W. Trucks, H.B. Schlegel, P.M.W. Gill, B.G. Johnson, M.A. Robb, J.R. Cheeseman, T.A. Keith, G.A. Petersson, J.A. Montgomery, K. Raghavachari, M.A. Al-Laham, V.G. Zakrzewski, J.V. Ortiz, J.B. Foresman, J. Cioslowski, B.B. Stefanov, A. Nanayakkara, M. Challacombe, C.Y. Peng, P.Y. Ayala, W. Chen, M.W. Wong, J.L. Andres, E.S. Replogle, R. Gomperts, R.L. Martin, D.J. Fox, J.S. Binkley, D.J. Defrees, J. Baker, J.J.P. Stewart, M. Head-Gordon, C. Gonzalez, J.A. Pople, GAUSSIAN 94, Revision B.1, Gaussian Inc., Pittsburgh, PA, 1995.
[18] G. Schaftenaar, Univ. of Nijmegen, URL: http://www.caos.kun.nl/~shaft/molden/molden.html.
[19] Copyright 1990, 1991, 1992, 1993 Research Equipment, Inc. d/b/a Minnesota Supercomputer Center, Inc.
[20] M.J. Locke, R.T. McIver, J. Am. Chem. Soc. 105 (1983) 4226.
[21] J.H. Jensen, M.S. Gordon, J. Am. Chem. Soc. 117 (1995) 8170.
[22] (a) Y. Ding, K. Krogh-Jespersen, Chem. Phys. Lett. 199 (1992) 261; (b) D. Yu, D.A. Armstrong, A. Rauk, Can. J. Chem. 70 (1992) 1762.
[23] (a) R.D. Brown, P.D. Godfrey, J.W.V. Storey, M.P. Bassez,

J. Chem. Soc. Chem. Commun. (1978) 547; (b) R.D. Suenram, F.J. Lovas, J. Mol. Spectrosc. 72 (1978) 372; (c) R.D. Suenram, F.J. Lovas, J. Am. Chem. Soc. 102 (1980) 7180; (d) K. Iijima, K. Tanaka, S. Onuma, J. Mol. Struct. 246 (1991) 257; (e) P.D. Godfrey, R.D. Brown, J. Am. Chem. Soc. 117 (1995) 2019; (f) I.D. Reva, A.M. Plokhotnichenko, S.G. Stepanian, A.Y. Ivanov, E.D. Radchenko, G.G. Sheina, Y.P. Blagoi, Chem. Phys. Lett. 232 (1995) 141; [Erratum] 235 (1995) 617; (g) P.D. Godfrey, R.D. Brown, F.M. Rodgers, J. Mol. Struct. 376 (1996) 65; (h) J.J. Neville, Y. Zheng, C.E. Brion, J. Am. Chem. Soc. 118 (1996) 10 533.

[24] (a) M. Ramek, V.K.W. Cheng, S.Q. Newton, L. Schäfer, J. Mol. Struct. 245 (1991) 12, and references cited therein; (b) J.H. Jensen, M.S. Gordon, J. Am. Chem. Soc. 113 (1991) 3917; (c) A.G. Csaszar, J. Am. Chem. Soc. 114 (1992) 9568; (d) R.F. Frey, J. Coffin, S.Q. Newton, M. Ramek, V.K.W. Cheng, F.A. Momany, L. Schäfer, J. Am. Chem. Soc. 114 (1992) 5369; (e) C.H. Hu, M. Shen, H.F. Schaefer III, J. Am. Chem. Soc. 115 (1993) 2923; (f) V. Barone, C. Adamo, F. Lejl, J. Chem. Phys. 102 (1995) 364; (g) S. Hoyau, G. Ohanessian, J. Am. Chem. Soc. 119 (1997) 2016; (h) D.T. Nguyen, A.C. Scheiner, J.W. Andzelm, S. Sirois, D.R. Salahub, D.T. Hagler, J. Comput. Chem. 18 (1997) 1609.

[25] K. Chung, R.M. Hedges, R.D. Macfarlane, J. Am. Chem. Soc. 98 (1976) 7523.

[26] L.R. Wright, R.F. Borkman, A. Gabriel, J. Phys. Chem. 86 (1982) 3951.

[27] F. Jensen, J. Am. Chem. Soc. 114 (1992) 9533.

[28] S. Bouchonnet, Y. Hoppilliard, Org. Mass Spectrom. 27 (1992) 71.

[29] J. Wu, C.B. Lebrilla, J. Am. Chem. Soc. 115 (1993) 3270.

[30] D.Y.A. Rauk, D.A. Armstrong, J. Am. Chem. Soc. 117 (1995) 1789.

[31] E. Uggerud, Theor. Chim. Acta 97 (1997) 313.

[32] K. Zhang, A. Chung-Phillips, J. Phys. Chem. A 102 (1998) 3625.

[33] K. Zhang, A. Chung-Phillips, J. Chem. Inf. Comput. Sci. 39 (1999) 382.

[34] K. Zhang, A. Chung-Phillips, J. Comput. Chem. 19 (1998) 1862.

[35] Z.B. Maksic, B. Kovacevic, Chem. Phys. Lett. 307 (1999) 497.

[36] M. Meot-Ner, E.P. Hunter, F.H. Field, J. Am. Chem. Soc. 101 (1979) 686.

[37] S.G. Lias, J.F. Liebman, R.D. Levin, J. Phys. Chem. Ref. Data 13 (1984) 695.

[38] G.S. Gorman, J.P. Speir, I.J. Amster, J. Am. Chem. Soc. 114 (1992) 3986.

[39] K. Zhang, D.M. Zimmerman, A. Chung-Phillips, C.J. Cassady, J. Am. Chem. Soc. 115 (1993) 10 812.

[40] G. Bojesen, J. Am. Chem. Soc. 109 (1987) 5557.

[41] K. Isa, T. Omote, M. Amaya, Org. Mass Spectrom. 25 (1990) 620.

[42] S.A. McLuckey, D. Cameron, R.G. Cooks, J. Am. Chem. Soc. 103 (1981) 1313.

[43] E.P. Hunter, S.G. Lias, NIST Standard Reference Database Number 69, W.G. Mallard, P.J. Linstrom (Eds.), National Institute of Standards and Technology, Gaitherburg, MD, 1998, or J. Phys. Chem. Ref. Data 27 (1998) 413.

[44] B.J. Smith, L. Radom, J. Am. Chem. Soc. 115 (1993) 4885.

[45] M.H. Lien, A.C. Hopkinson, J. Org. Chem. 53 (1988) 2150.

[46] W.D. van Dongen, W. Heerma, J. Haverkamp, C.G. de Koster, Rapid Commun. Mass Spectrom. 10 (1996) 1237.

[47] J.L. Holmes, A.A. Mommers, J.K. Terlouw, C.E.C.A. Hop, Int. J. Mass Spectrom. Ion Processes 68 (1986) 249.

[48] S.G. Lias, J.E. Bartmess, J.F. Liebman, J.L. Holmes, R.D. Levin, W.G. Mallard, J. Phys. Chem. Ref. Data 17 (1988) 1 (suppl).

[49] (a) P.C. Burgers, A.A. Mommers, J.L. Holmes, J. Am. Chem. Soc. 105 (1983) 5976; (b) F.A. Wiedmann, J. Cai, C. Wesdemiotis, Rapid Commun. Mass Spectrom. 8 (1994) 804.